JOURNAL OF CATALYSIS **112**, 135–144 (1988)

A Transient Infrared and Isotopic Study of Methanation over Ni/Al_2O_3

D. M. STOCKWELL, J. S. CHUNG, AND C. O. BENNETT

Department of Chemical Engineering, University of Connecticut, Storrs, Connecticut 06268

Received March 4, 1987; revised January 25, 1988

Methanation of CO/H_2 mixtures over a 10% Ni/Al_2O_3 catalyst has been studied by infrared spectroscopy and several isotopic techiques. Emission spectra revealed the presence of both linear and bridge-bonded CO during reaction, but no reactive H–C–O or C–H species were observed. Isotopic substitution experiments were conducted in a gradientless microreactor. These show that a heterogeneous layer of CH_x also accumulates. The probable value of x is zero. As much as 0.6 monolayer has been observed, but the amount depends on the reaction conditions. The global rate of methanation is controlled by a competition between the formation and the hydrogenation of this species, not by a single rate-determining step.

INTRODUCTION

The methanation of CO is generally considered to proceed by the dissociative mechanism on most reduced metal surfaces, on the basis of a number of investigations reported in the literature (*1–7*). Experiments, mostly with ^{13}C-labeled CO, have also shown that the coverage of active CH_x species is usually a significant, measurable quantity (*5–11*). Working between 210 and 260°C with Ni/SiO_2 and Raney Ni catalysts, Yang *et al.* (*10, 11*) found that the steady-state value of θ_{CH_x} is independent of H_2/CO ratio, but increases with temperature. They concluded that θ_{CH_x} is controlled by the density of active sites and that the sole rate-limiting step is the hydrogenation of CH_x.

In contrast to these findings, other studies of methanation on a Ni/Al_2O_3 catalyst indicate that two steps in series are important in determining θ_{CH_x} and the rate of reaction (*12, 13*). The amount of CH_x present was found to increase slowly with time on stream at a rate which paralleled the approach to steady-state methanation (*13*). In the present study we find that the coverage of CH_x is also influenced by the H_2/CO ratio. It does not appear to be restricted to a small portion of active sites. Why these catalysts differ so from Ni/SiO_2 and Raney Ni catalysts (*11*) is not understood, but it is interesting considering the supposed inertness of these supports.

The purpose of this work was to characterize the methanation reaction for our Ni/Al_2O_3 catalysts, both for its own sake and in preparation for a study of chain growth under the same conditions (*14*). For completeness and ease of interpretation, we have conducted our experiments in a gradientless microreactor at low conversion. The compartmental modeling scheme of Happel *et al.* (*8, 15*) is used in support of some of our results. In summary, we shall present evidence that the rate-controlling steps in methanation are the dissociation of *CO and the hydrogenation of $*CH_x$ with the population of $*CH_x$ controlled by these two steps. In the intermediate CH_x, the probable value of x is zero, for our reaction system.

METHODS

Materials. The catalysts were each 10 wt% Ni/Al_2O_3 prepared by the incipient wetness technique. Two batches of catalyst were used. Sample A was prepared by Underwood and used in previous studies (*13, 16*). With this sample in short supply, we also made use of Sample B, prepared by Borcar. The starting materials and preparation methods in each case were the same.

0021-9517/88 $3.00

Alon-C (Degussa) was impregnated to incipient wetness with an appropriate aqueous solution of $Ni(NO_3)_2$. The catalyst was dried, pelletized, and screened to give 0.59- to 1.18-mm particles. All samples were reduced *in situ* by slowly heating under 1 atm flowing of H_2, following Bartholomew and Farrauto (*17*). There was a 1-h hold at 230°C, and the catalysts were maintained at 450°C for 16 h or more.

Hydrogen chemisorption has shown that the fraction of Ni atoms exposed is about 0.2, equivalent to 321 μmol of Ni atoms per gram of supported catalyst. By X-ray line broadening the particle size is about 4.6 nm, consistent with the chemisorption result. The reduction conditions used should lead to at least 95% reduction of the Ni (*17*). The BET area of the supported catalyst is 117 m^2/g.

Gases were premixed from standard grade components as before (*13*). Isotopically labeled mixtures were prepared using 91.91% ^{13}CO (MSD) or 99.5% D_2 (Matheson). The ^{13}CO contained 7.66% ^{17}O and 8.25% ^{18}O. The flow rates of these gases were always 30 cc/min (ambient). Instruments were calibrated against known mixtures several times each day. Varying H_2/CO ratios at 1 atm were made by keeping the CO partial pressure at 0.1 atm and replacing the appropriate part of the H_2 by He.

Reactor. Figure 1 shows the reactor. A shallow, wide bed is used in the reactor in order to promote backmixing by diffusion and eddy effects (*18*). For the flow rates used here, and taking the characteristic length to be the length of the chamber itself, we obtain Peclet numbers close to unity, based on dispersion by molecular diffusion. In order to enhance the backmixing effect via eddies, the gas inlet tube was sealed over at the end, and two small holes were drilled in from the side. Another was drilled at the end but placed off center. The material of construction was 304 stainless steel.

Flow system. The flow system used was similar to those described earlier (*19*), with

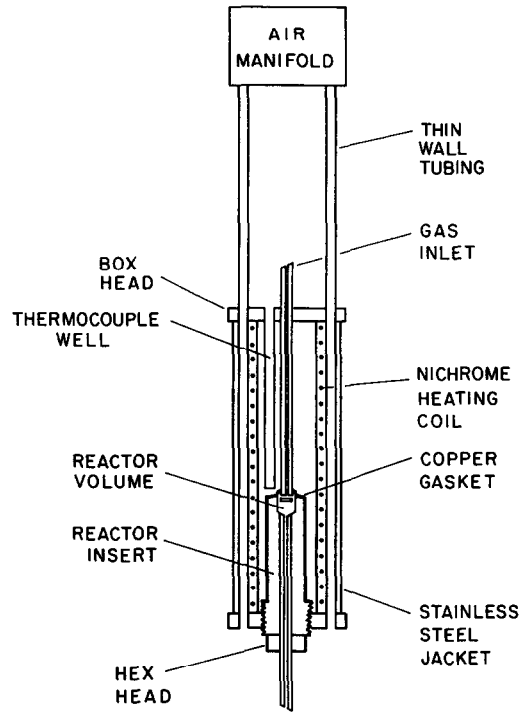

FIG. 1. Reactor for transient kinetic studies. Power for the heating coil was supplied by leads through the top surface.

the important addition of a gas chromatograph for hydrocarbon analysis (*14*). Concentration and isotopic transients were monitored with a high-resolution, magnetic sector type mass spectrometer (Nuclide 12-90-G) set at a resolution of about 500. Significantly, this allowed the exclusion of $^{16}OH^+$ and $^{17}O^+$ from the $^{13}CH_4^+$ ion beam, $^{16}O^+$ from the $^{12}CH_4^+$ ion beam, $D_2^{16}O^+$ from the $^{12}CD_4^+$ ion beam, and He^{2+} from the H_2^+ ion beam. Beam currents were measured with an AEM-1000 electron multiplier (Vacumetrics), followed by an electrometer (RC = 0.1 s) and a MINC 11 microcomputer (DEC). The circuit was designed to give a linear dynamic range of 10^5 and a signal-to-noise ratio limited only by statistical fluctuations. In order to obtain these results, we sacrificed speed. All transients were therefore recorded one peak at a time, and repeated as necessary (*13*).

Infrared measurements. The infrared apparatus has been described (*19*). The emission mode was used and spectra were recorded under reaction conditions. Special precautions were taken to ensure that thermal transients in the gas phase above the catalyst were not important.

RESULTS AND DISCUSSION

Infrared spectroscopy. Figure 2 shows the emission from a 3.5-mg sample (1-cm^2 disk) of catalyst at 220°C. During reaction under 4.4% CO/22% H_2/He, there are comparable amounts of both linear and bridge-bonded CO. When the feed gas was switched to He, part of the CO slowly desorbed from both states. Figure 2 also shows adsorbed CO before and after a switch from $^{12}CO/H_2$ to $^{13}CO/H_2$. The surface CO was exchanged rapidly with a time constant of about 2 s, but it is difficult to obtain meaningful spectra during the transient (*5*).

The traces of selected wavenumbers during the sequence $H_2 \rightarrow CO/H_2 \rightarrow He \rightarrow H_2$ have been followed at 220°C. As was reported earlier (*13*), CO adsorbs rapidly, but is removed only slowly by purging with He. The results after a switch to H_2 indicate that the titration kinetics are quite complicated, but in any event all the surface CO was removed within 30 s after the switch to H_2.

We also observed bands at 1455 and 1583 cm^{-1}. These bands increased slowly with time on stream and were most pronounced at low H_2/CO ratios. Reduction at 370°C for

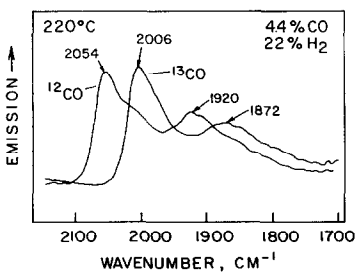

FIG. 2. Infrared spectra of labeled CO on 10% Ni/Al_2O_3 during reaction at 220°C.

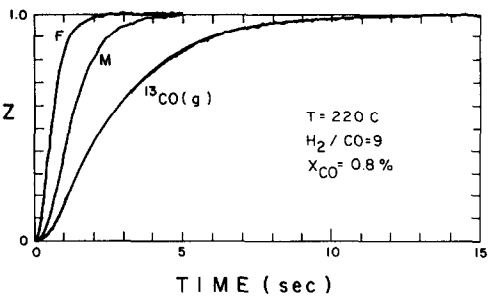

FIG. 3. Experimental forcing (F), mixing (M), and ^{13}CO curves under reaction conditions. The simulation of ^{13}CO with $\tau_0 = 2.3$ is also shown.

8 h was required for their removal; thus the species are not reaction intermediates. We attribute them to acetaldehyde adsorbed on the support (*20, 21*). Trace quantities of acetaldehyde were detected in the products. No bands were observed in the C–H region of 3100–2700 cm^{-1} at 220°C and $H_2/CO = 9$. Under these conditions, the acetaldehyde band was very weak, but about 0.15 monolayer of CH_x was present on the catalyst.

Forcing, mixing, and CO exchange. We turn now to some experiments in the microreactor, with concentration analysis by continuous inlet mass spectrometry. Curves (F) and (M) of Fig. 3 show the dimensionless transient response of argon after a switch from 9.9% ^{12}CO/1% He/89.1% H_2 to 9.9% ^{13}CO/1% Ar/89.1% H_2. The results are reported in terms of a normalized, dimensionless variable Z, defined as

$$Z = \frac{y - y_0}{y_\infty - y_0}, \qquad (1)$$

where y_0 and y_∞ refer to the mole fractions at $t = 0$ and $t \rightarrow \infty$. Data were collected at 60 Hz, 220°C, and using an 18-mg sample of Ni/Al_2O_3 catalyst B. To obtain the forcing function, a six-way gas chromatographic valve was switched to bypass the reactor. The bypass loop on the valve was made of the same tubing and fittings as those leading to the reactor and was strapped to the outside of the reactor to maintain it close to

reaction temperature. In this way, the forcing function accounted for all of the backmixing and electronic time delays outside of the reactor. To show that the reactor is gradientless, we compare our mixing curve to the response of an ideal CSTR by the procedure that follows.

The forcing function is not a perfect step, so it must be fit empirically. We use a dimensionless series of exponentials

$$Z^{\mathrm{f}} = 1 - \sum_{p}^{N} b_p\, e^{-a_p t} \quad (t > 0) \qquad (2)$$

which, among other things, represents a series of N unequally sized CSTRs. This function may then be applied to a final CSTR, and the output compared to the experimental mixing curve. If the reactor is truly gradientless, then the simple kinetic analysis described by Happel *et al.* (*15*) may be applied.

We require the response of an ideal CSTR to the forcing function Eq. (2). A material balance for a gradientless reactor, with y the mole fraction of Ar and τ_{m} the mixing time, gives

$$y^{\mathrm{f}} = y + \tau_{\mathrm{m}} \frac{dy}{dt} \qquad (3)$$

with y^{f} representing the forcing function. Substituting in terms of Z gives

$$Z^{\mathrm{f}} = Z + \tau_{\mathrm{m}} \frac{dZ}{dt}. \qquad (4)$$

When the forcing function is Eq. (2), the solution is

$$Z = 1 + \sum_{p=1}^{N} \left(\frac{+b_p}{1 - a_p \tau_{\mathrm{m}}} \right) e^{-a_p t} + \left[-1 + \sum_{p=1}^{N} \left(\frac{-b_p}{1 - a_p \tau_{\mathrm{m}}} \right) \right] e^{-t/\tau_{\mathrm{m}}}. \qquad (5)$$

Since the general form remains the same, it is a simple matter to assemble the numerical values of the coefficients for a series using a small computer.

The experimental forcing function curve (F) of Fig. 3 has been fit by Eq. (2), and an excellent fit is obtained by coefficients which are equivalent to three small CSTRs. Then Eq. (5) is used for the added CSTR, and the curve (M) of Fig. 3 is fit well by $\tau_{\mathrm{m}} = 0.73$ s for this CSTR, which represents the microreactor response. The reactor volume calculated from this time is 0.59 cc, which agrees well with the geometric volume estimated as 0.5 cc.

The departure of the forcing function from a step function arises from time effects occurring in the switching valve, the sampling lines, and the response of the mass spectrometer. Some of these effects act after the reactor and others before, but they can all be treated together and considered one forcing function. This is so because they and the reactor are all represented by linear differential equations. The transfer functions are multiplied together, so order is irrelevant.

The observed mixing curve has some S-shape to it; however, this is all accounted for by the three CSTRs of the forcing function. The reactor itself responds as a single CSTR.

The third curve of Fig. 3 represents the $^{13}CO(g)$ response. The area between this curve and the mixing curve (M) is proportional to the amount of $^{12}CO^*$ initially present on the catalyst surface and which has been replaced by $^{13}CO^*$. To interpret this curve, consider a gradientless reactor running at steady state with a certain feed of H_2/CO. The feed rate of CO is R_{F}, the conversion of CO to products is X_{CO}, and the rates of adsorption and desorption are R_+ and R_-, respectively. There are $N_{\mathrm{CO(g)}}$ gaseous CO molecules and $N_{\mathrm{CO^*}}$ adsorbed CO molecules in the reactor. Then a balance on $^{13}CO(g)$ yields

$$Z^{\mathrm{f}} + \beta Z_{\mathrm{CO^*}} = (1 + \beta) Z_{\mathrm{CO(g)}} + (1 + \beta) \tau_{\mathrm{CO(g)}} \frac{dZ_{\mathrm{CO(g)}}}{dt}, \qquad (6)$$

where $\beta = R_-/R_{\mathrm{F}}$. A balance on $^{13}CO^*$ gives

$$Z_{CO(g)} = Z_{CO^*} + \tau_{CO^*} \frac{dZ_{CO^*}}{dt}, \quad (7)$$

where

$$\beta = \frac{R_-}{R_F}, \quad (8a)$$

$$\tau_{CO(g)} = \frac{N_{CO(g)}}{R_F + R_-}, \quad (8b)$$

$$\tau_{CO^*} = \frac{N_{CO^*}}{X_{CO} R_F + R_-}. \quad (8c)$$

In these equations, Z is defined similarly to Eq. (1), with y taken to be the atom fraction ^{13}C. The initial and final values of Z are thus 0 and 1.0. The system of equations is most easily solved by Laplace transform methods (*22*), and Soong *et al.* (*23*) discuss a related solution.

Although the equations appear complicated, we can understand much without obtaining their solution. If the exchange rate β is zero, Eq. (6) is independent of Eq. (7) and $Z_{CO(g)}$ approaches the mixing curve for small X_{CO}. For $\beta \to \infty$ we have $\tau_{CO^*} \to 0$, and by Eq. (7), $Z_{CO(g)} = Z_{CO^*}$. Combining Eqs. (6) and (7) for this case yields

$$Z^f = Z_{CO} + \left(\frac{N_{CO^*} + N_{CO(g)}}{R_F}\right) \frac{dZ_{CO}}{dt} \quad (9)$$

so that the combined pools behave as one CSTR with time constant

$$\tau_0 = \frac{N_{CO^*} + N_{CO(g)}}{R_F}. \quad (10)$$

It is interesting to consider a simulation of how the variation of β would affect the observed response of $^{13}CO(g)$ and the corresponding response of $^{13}CO^*$. Figure 4 shows the expected behavior for $X_{CO} = 0.05$ and $N_{CO^*}/(N_{CO^*} + N_{CO(g)}) = 0.83$, representative of the conditions used in the experiments.

The $^{13}CO(g)$ curve of Fig. 3 can now be interpreted. Since R_F, X_{CO}, and $N_{CO(g)}$ are known, we search for the values of β and N_{CO^*} which fit the data. The best fit, which is shown in Fig. 3, corresponds to $\beta \to \infty$, and the amount of surface CO is 172 μmol/g, corresponding to $\theta = 0.53$. The value of τ_0 in Eq. (10) is 2.3 s, and of course $Z_{CO^*} = Z_{CO(g)}$. This result of rapid CO exchange agrees with previous studies on Ni, Ru, and Co (*4–6, 8–11*). It is also consistent with the gradientless behavior of the reactor.

Surface carbon and methanation. After reaction in CO/H_2, a switch to H_2 produces a peak in CH_4 production attributable to the reduction of CH_x and CO* (*13*). In order to deconvolute this combined response, the following experiment was conducted.

After reaction in $^{12}CO/H_2$, a switch was made to $^{13}CO/He$, and then to H_2. During the 20-s exposure to $^{13}CO/He$, the $^{12}CO^*$ was replaced with $^{13}CO^*$ and the methanation reaction was rapidly quenched (*13*). A few micromoles per gram of $^{12}C + {}^{13}C$ were deposited via the Boudouard reaction, but this quantity is negligible. The methane peak produced in H_2 was therefore labeled;

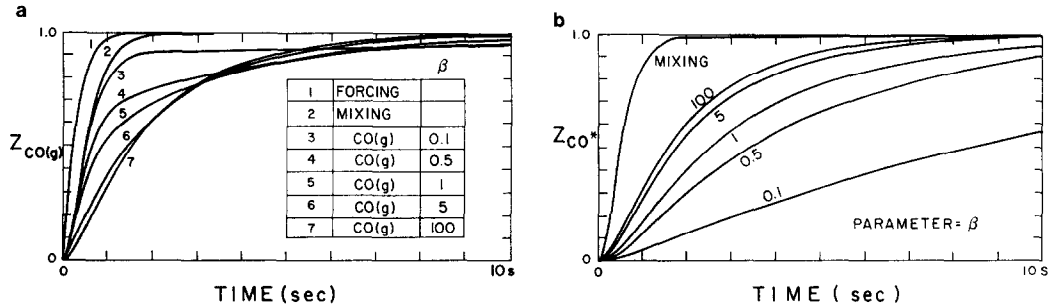

FIG. 4. Simulation of CO exchange using parameters from a previous study (*16*). (a) $Z_{CO(g)}$; (b) Z_{CO^*}.

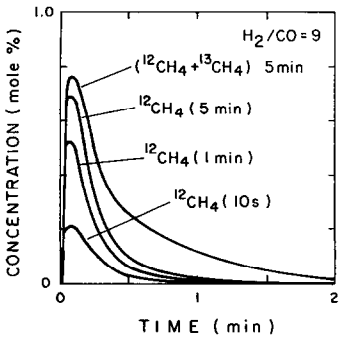

FIG. 5. Growth of the $^{12}CH_4$ ex $^{12}CH_x$ peak in H_2 with time on stream. Parameter is time in $^{12}CO/H_2$ at 220°C.

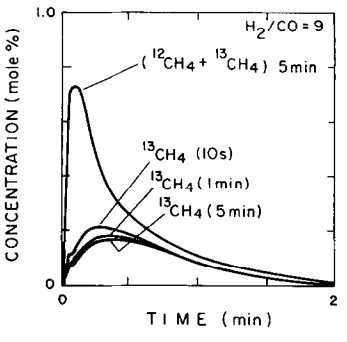

FIG. 6. Decline in $^{13}CH_4$ ex $^{13}CO^*$ titrated in H_2 as time on stream was increased at 220°C.

$^{12}CH_4$ was produced by reduction of $^{12}CH_x$ and $^{13}CH_4$ was produced by reduction of $^{13}CO^*$. Corrections for the ^{12}CO impurity in the ^{13}CO/He mixture were made, but not for the natural 1.1% abundance of ^{13}C in $^{12}CO/H_2$. The cracking pattern for $^{13}CH_4$ ex ^{13}CO was established by methanation of the ^{13}CO in the GC-MS system described elsewhere (*14*) and measurements were made using the m/e = 16 and 17 peaks.

Figure 5 shows the results obtained at 220°C, H_2/CO = 9, and varying times on stream. As has been discussed previously (*13*), the quantity of CH_x on the catalyst increases slowly with time on stream until a steady state is reached. In Fig. 6 we observe that the quantity of $^{13}CH_4$ ex ^{13}CO titrated decreased somewhat with time on stream. Table 1 summarizes the quantities obtained in each case. When the deconvolution is checked by comparing the amounts of $^{12}CH_4$ + $^{13}CH_4$ to the $^{12}CH_4$ produced during the sequence $^{12}CO/H_2 \rightarrow$ ^{12}CO/He $\rightarrow H_2$, the results always agree to within 5%. The coverages of CO* in this table are smaller than the 172 μmol/g obtained from Fig. 3. The curve of ^{13}CO after the switch ^{13}CO/He $\rightarrow H_2$ has been measured and found to lie above the decay expected from gas-phase replacement in the mixed reactor. On the order of 40 μmol ^{13}CO/g desorbs before the $^{13}CO^*$ can dissociate and react with surface hydrogen to form methane; thus the values of $^{13}CO^*$ on the order of 100–135 μmol/g from Table 1 are consistent with the 172 μmol/g obtained from Fig. 3.

Figure 7 compares the $^{12}CH_4$ peaks obtained after reaction in H_2/CO = 1 and H_2/CO = 9 at 220°C. Both experiments represent a steady-state surface, but the time required to reach it under H_2/CO = 1 is much longer. The quantity of CH_x present under H_2/CO = 1 is larger, and the shape of the peak shows that the carbon is still very reactive. The quantities found are given in the last line of Table 1.

Results similar to those of Table 1 have been measured at 250°C also, and the coverages of both CO* and CH_x are about 0.75 times those at 220°C. The time on stream for both cases is 5 min. Yang *et al.* (*10*)

TABLE 1

Quantities of CH_x and CO* by ^{13}CO/He titration at 220°C

Time on stream	H_2/CO	$^{12}CH_x$	$^{13}CO^*$	θ_{CH_x}[a]
10 s	9	45	132	0.1
1 min	9	96	120	0.3
5 min	9	142	114	0.4
5 min	9	131	107	0.4
25 min	1	197	101	0.6

Note. Amounts given in micromoles per gram catalyst B.

[a] Based on 321 μmol Ni_{surf}/g.

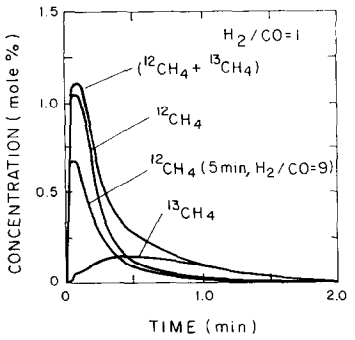

FIG. 7. Isotopic deconvolution of H_2 titration curve after 25 min on stream in $H_2/CO = 1$ at 220°C. Also shown is $^{12}CH_4$ ex $^{12}CH_x$ from 5 min $^{12}CO/H_2$ at 220°C, $H_2/CO = 9$.

found increases in coverage with temperature for the CO/H_2 reaction over Raney Ni and over Ni/SiO_2.

The coverages of CH_x and CO* are also sensitive to the ratio H_2/CO. The sensitivity of the surface coverages to H_2/CO, temperature, and time on stream gives evidence that these coverages are the result of a balance between the rates of CO dissociation and C hydrogenation, as suggested by Goodman *et al.* (*12*). This balance is apparently also affected by changes in the support, a possible explanation of the differences noted above between our results and those of Yang *et al.* (*10*). The trends in θ_{CH_x} and θ_{CO} found here are in general agreement with single crystal studies (*12, 24, 25*).

In order to discover what other forms of carbon might be present on the catalyst during reaction, a temperature-programmed reduction (TPR) of the catalyst was run after the reactive CH_x and CO* had been removed. Small amounts of unreactive coke were found after reaction at temperatures between 220 and 275°C, and H_2/CO ratios between 1 and 9. The amount increased monotonically with time on stream, but the time scale for accumulation is much longer than that of the rise to steady state. The rate of carbon deposition appeared to be nearly independent of H_2/CO ratio, and to increase with increasing temperature. The coke was stable with respect to reduction at reaction temperature over a period of 24 h.

Figure 8 gives some TPRs after increasing times on stream. The CO/H_2 reaction was performed 275°C and $H_2/CO = 9$, and the ramp was begun after 30 s of H_2 exposure. The peaks at 616 and 748 K were produced by the reduction of coke on the catalyst. Some portion of the 748 K peak and most of the CH_4 produced above 800 K was due to the reduction of some form(s) of carbon in or on the steel walls of the reactor. Since the ratio of the nickel area to the wall area was on the order of 10^3, filamentous or bulk carbon is expected. The reactor itself has no measurable catalytic activity. Even with this other carbon included, a maximum of only about 0.1 monolayer of coke was found. Coke accumulations of many monolayers are possible on Ni catalysts (*6, 23*), but for short times on stream under these conditions, our catalysts are relatively clean.

More information about the nature of the surface CH_x species can be obtained by a steady-state tracing experiment such as that leading to Fig. 3. However, now we follow the $^{13}CH_4$ response, as shown in Fig. 9, at 250°C for $H_2/CO = 5$, and 5 min on stream. The conversion of CO was 0.9%, the methane turnover frequency was 4.1 ×

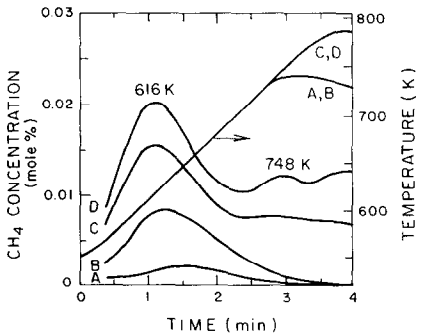

FIG. 8. TPR in H_2 of unreactive coke accumulated under $H_2/CO = 9$ at 275°C. Times on stream were (A) 1 min, (B) 5 min, (C) 12 min, (D) 25 min. The amount under curve D is 33 μmol/g.

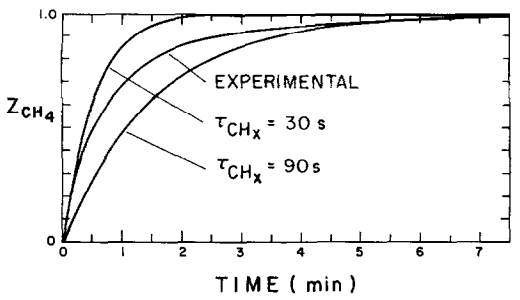

FIG. 9. Response of $^{13}CH_4$ after the switch from $^{12}CO/H_2$ to $^{13}CO/H_2$ at 250°C, $H_2/CO = 5$, and 5 min on stream. Also shown are two homogeneous pool models for the time constants indicated. The total amount of CH_x found is 96 μmol/g.

10^{-3} s^{-1}, the selectivity to methane was 82% of all organic carbon, and the Shultz–Flory–Anderson parameter α was 0.26. Under these conditions, a CO exchange experiment like those of Figs. 5–7 gave a total CH_x quantity of 101 μmol/g.

From Fig. 9 we note that the $^{13}CH_4$ response is slow compared to the ^{13}CO response of Fig. 3. In addition to the experimental result, plotted in Fig. 9 are curves for a homogeneous pool which would fit the first part of the curve (τ_{CH_x} = 30 s) or the final part of the curve (τ_{CH_x} = 90 s). The surface CH_x is thus nonuniform. Many models can be proposed to represent this behavior, which has been observed for various metals (*6, 23, 26*). Soong *et al.* (*23*) consider two pools, one of active carbon, another of less active carbon. These pools can be modeled as two CSTRs connected in various ways, but the agreement with the experimental result is not sensitive to several of the manners of connection. De Pontes *et al.* (*27*) have successfully modeled the data of Soong *et al.* (*23*) by finding the distribution of reactivities (k) of a large number of parallel pools which would give the observed result.

We have fit one of the models of Soong *et al.* (*23*) to the data of Fig. 9. Good results are obtained with a pool of 48 μmol/g of more active CH_x which exchanges at a finite rate with an equally sized less active pool. However, in view of the insensitivity of the fit to the various models, it does not seem profitable to analyze Fig. 9 in any more detail.

The total amount of CH_x derived from Fig. 9 is 96 μmol/g, close to the value of 101 μmol/g found by the CO* exchange experiment. The total CH_x obtained from Fig. 9 arises from a material balance and does not depend on a model.

In order to gain information about the value of x in CH_x, a steady-state tracing experiment using the switch $CO/H_2 \rightarrow CO/D_2$ was performed, and the result is shown in Fig. 10. The HD has disappeared by the time the D_2 trace shown reaches 1.0, and the CD_4 peak rises rapidly thereafter. This result could mean that $x = 0$ in the CH_x surface species, if the H in CH_x were not exchangeable. However, it is possible that the exchange of surface H* to D* and then of surface CH_x to CD_x is very fast and produces a peak of H_2 which would be undetectable in the large H_2 flow at time zero ($H_2/CO = 9$). Thus it can be said that the result of Fig. 10 is necessary if x is to be zero, but not sufficient to prove that $x = 0$.

Hydrogen spillover and exchange of D with the OH of the support would also lead to the transient production of H_2, HD, and the less deuterated methanes. We suspect that this exchange is very rapid at 250°C so that these peaks are not detectable. All of them should be past by the time $Z_{CD_4} = 1.0$. Other experiments show that exchange

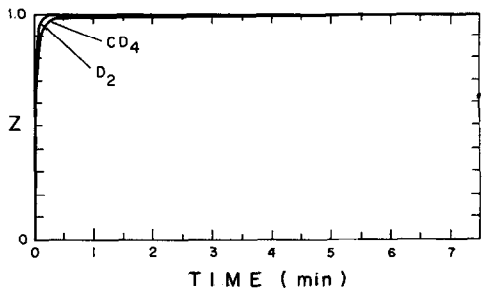

FIG. 10. Response of CD_4 to the switch $^{12}CO/H_2 \rightarrow {}^{12}CO/D_2$ after 5 min on stream. Same conditions as in Fig. 9.

with the support via spillover is occurring. A switch from H_2 to He at 250°C desorbs all the H_2 from the Ni/Al_2O_3 catalyst. Then a switch to D_2 produces a peak of HD; the H must come from the support. Similarly, a washing experiment was done as follows.

Carbon is deposited on the catalyst via 10% CO in He, and then a switch is made to He. Upon subsequently switching to D_2, a nice CHD_3 peaks appears. The H has come from the support. Tanaka *et al.* (*28*) find a similar result for supported cobalt catalysts, and the same kind of result is obtained on iron catalysts (*29*).

Happel *et al.* (*8, 15, 26*) using the switch $CO/H_2 \rightarrow CO/D_2$ claim that there is abundant CH_1 on their Ni catalyst during the CO/H_2 reaction. However, in their experiment it requires about 6 min to replace the H_2 by D_2, so surface CH_x is reacting with both H* and D* during this period. Their modeling takes this into account, but the results would be more convincing if the gas-phase volume were small so that the deuterated peaks might appear well after the replacement of H_2 by D_2.

It has previously been reported (*13*) that $x = 0$ in CH_x because it was found that an oxygen titration of the surface after a switch from CO/H_2 to He produces no H_2O. In the present work we have also found no IR bands in the C–H stretching region during reaction under the conditions of Fig. 2. In view of the preceding discussion, the most probable value of x seems to be zero.

CONCLUSIONS

During the methanation of CO on 10% Ni/Al_2O_3 the surface is covered by both CH_x and adsorbed CO, as detailed in Table 1. The ratio of θ_{CH} to θ_{CO} increases with time on stream and with CO/H_2 ratio. The surface state depends on both the rate of CO dissociation and the rate of CH_x hydrogenation without a well-defined rate-controlling step. The results of steady-state tracing and surface titration via CO* exchange are in general agreement.

The surface CH_x species is nonuniform; parts of it exchange their ^{12}C to ^{13}C more quickly than other parts. The evidence from steady-state tracing via D_2 and other experiments indicates that the value of x in CH_x is probably zero.

REFERENCES

1. Wentrcek, P. R., Wood, B. J., and Wise, H., *J. Catal.* **43,** 363 (1976).
2. Araki, M., and Ponec, V., *J. Catal.* **44,** 439 (1976).
3. Rabo, J. A., Risch, A. P., and Poutsma, M. L., *J. Catal.* **53,** 295 (1978).
4. Biloen, P., Helle, J. N., and Sachtler, W. M. H., *J. Catal.* **58,** 95 (1979).
5. Cant, N. W., and Bell, A. T., *J. Catal.* **73,** 257 (1982).
6. Biloen, P., Helle, J. N., van den Berg, F. G. A., and Sachtler, W. M. H., *J. Catal.* **81,** 450 (1983).
7. Bianchi, D., Borcar, S., Teule-Gay, F., and Bennett, C. O., *J. Catal.* **82,** 442 (1983).
8. Happel, J., Suzuki, I., Kokayeff, P., and Fthenakis, V., *J. Catal.* **65,** 59 (1980).
9. Kobori, Y., Yamasaki, H., Naito, S., Onishi, T., and Tamaru, K., *J. Chem. Soc. Faraday Trans. 1* **78,** 1473 (1982).
10. Yang, C.-H., Soong, Y., and Biloen, P., "Proceedings, 8th International Congress on Catalysis, Berlin, 1984," Vol. II, p. 3. Dechema, Frankfurt-am-Main, 1984.
11. Yang, C.-H., Soong, Y., and Biloen, P., *J. Catal.* **94,** 306 (1985).
12. Goodman, D. W., Kelley, R. D., Madey, T. E., and White, J. M. *J. Catal.* **64,** 479 (1980).
13. Underwood, R. P., and Bennett, C. O., *J. Catal.* **86,** 245 (1984).
14. Stockwell, D. M., and Bennett, C. O., *J. Catal.* **110,** 354 (1988).
15. Happel, J., Cheh, H. Y., Otarod, M., Ozawa, S., Severida, A. J., Yoshida, T., and Fthenakis, V., *J. Catal.* **75,** 314 (1982).
16. Stockwell, D. M., and Bennett, C. O., "Preprints, ACS Division Petroleum Chemistry, Inc." Vol. 29, p. 543. Amer. Chem. Soc., Washington, DC 1984.
17. Bartholomew, C. H., and Farrauto, R. J., *J. Catal.* **45,** 41 (1976).
18. Zielinski, J., *React. Kinet. Catal. Lett.* **17,** 69 (1981).
19. Bennett, C. O., *in* "Catalysis under Transient Conditions" (A. T. Bell and L. L. Hegedus, Eds.), ACS Symposium Series, Vol. 178, p. 1. Amer. Chem. Soc., Washington, DC, 1982.
20. Naito, S., Yoshioka, H., Orita, H., and Tamaru, K., "Proceedings, 8th International Congress on

Catalysis, Berlin, 1984," Vol. 3, p. 207. Dechema, Frankfurt-am-Main, 1984.
21. Orita, H., Naito, S., and Tamaru, K., *J. Catal.* **90,** 183 (1984).
22. Wylie, C. R., "Advanced Engineering Mathematics," 4th ed. McGraw–Hill, New York, 1975.
23. Soong, Y., Krishna, K., and Biloen, P., *J. Catal.* **97,** 330 (1986).
24. Goodman, D. W., Kelley, R. D., Madey, T. E., and Yates, J. T., Jr., *J. Catal.* **63,** 226 (1980).
25. Kelley, R. D., and Semancik, S., *J. Catal.* **84,** 248 (1983).
26. Otarod, M., Ozawa, S., Yin, F., Chew, M., Cheh, H. Y., and Happel, J., *J. Catal.* **84,** 156 (1983).
27. De Pontes, M., Yokomizo, G. H., and Bell, A. T., *J. Catal.* **104,** 147 (1987).
28. Tanaka, K., Yaegaski, I., and Aomura, K., *J. Chem. Soc., Chem. Commun.,* 938 (1982).
29. Tau, L. M., and Bennett, C. O., *J. Catal.* **89,** 327 (1984).